

## Legendre spectral element method for seismic analysis of dam-reservoir interaction

R. Tarinejad\*, S. Pirboudaghi

Received: January 2014, Revised: April 2014, Accepted: April 2014

### Abstract

*It is well-known that dam-reservoir interaction has significant effects on the response of dams to the earthquakes. This phenomenon should be considered more exactly in the seismic design of dams with a rational and reliable dynamic analysis method. In this research, seismic analysis of the dam-reservoir is studied as a wave propagation problem by using Legendre Spectral element method (SEM). The special FEM and SEM codes are developed to carry out the seismic analysis of the dam-reservoir interaction system. The results of both SEM and FEM models are compared considering the accuracy and the time consumption of the analysis. Attractive spectral convergence of SEM is obtained either by increasing the degree of the polynomials in the reservoir or by the number of elements of dam. It is shown that all boundary conditions of the reservoir domain in the SEM are evaluated by the exact diagonal matrices. The SEM leads to the diagonal mass matrix for both dam and reservoir domains. The stiffness matrices obtained from the SEM are more sparse than the corresponding stiffness matrices in the FEM consequently the SEM needs a significant less time consumption of the analysis.*

**Keywords:** Spectral element method (SEM), Dam-reservoir interaction, Wave propagation, Finite element method (FEM), GLL quadrature.

### 1. Introduction

Wave propagation is a common phenomenon that appears in many applications. Distribution of hydrodynamic pressure during earthquakes in the reservoir of dams governed by Helmholtz equation is an acoustic wave propagation problem. The estimation of precise hydrodynamic forces on the dam faces due to earthquakes is an important safety aspect in the analysis and design of the dams. On the other hand, economically, it is not possible to consider all safety issues. Therefore, to satisfy both economic and safety considerations simultaneously, an analysis should be conducted to select the better and more accurate approach.

The analysis techniques have been enhanced considering the improved capabilities of computer processors and increased memory storage. The flexibility of the finite element method has motivated researchers to apply this technique in the analysis of dam-reservoir systems. For efficient numerical solution of the system, the unbounded reservoir is truncated at a certain distance away from the dam. Accuracy in the results can be obtained by truncating the infinite reservoir at a larger distance away from the dam. However, this results in an increased cost of computation.

There are numerous studies in dynamic analysis of dams considering water-structure interaction. The hydrodynamic pressure on vertical rigid structure subjected to ground motion was first solved analytically by Westergaard [1]. The added-mass method originated from his paper has influenced the engineering design of dams. Since then, many contributions to this subject have been reported. In 1967, Chopra [2] developed an analytical formulation for the hydrodynamic pressure of compressible water on a rigid dam with a vertical upstream face under both horizontal and vertical earthquake excitation. As the dam is assumed to be rigid in these studies, the effects of dam-reservoir interaction cannot be considered. Chakrabarti and Chopra [3] studied the effects of flexible gravity dam-reservoir interaction by employing the first few modes of vibration of the dam obtained with an empty reservoir. Chopra and Chakrabarti[4], Hall and Chopra [5], Fenves and Chopra[6] considered this issue in frequency domain by finite elements. Analysis in the time domain was considered by Sharan[7].

Spectral element method (SEM) is a highly accurate numerical method for wave propagation problems extensively studied and used in many engineering fields such as computational fluid dynamics [8], seismology [9], structural dynamics [10,11], etc.

Spectral method, as a conventional numerical method for partial differential equation, was first developed by Navier for problems of elastic sheet in the 1820s. However, due to its large amount of calculation, it was

\* Corresponding author: r\_tarinejad@tabrizu.ac.ir  
1 Assistant Professor, Faculty of Civil Engineering, University of Tabriz, Tabriz, East Azerbaijan Province, Iran

only used for single region problems in early period. In 1984, Patera [8] extended spectral method to many sub regions (or elements) by partitioning the given computational domain. By combining the spectral method with the finite element method, he initiated the idea of the spectral element method. Its development was the result of combining the accuracy and rapid convergence of the pseudo-spectral methods with the geometrical flexibility of the FEM. Chebyshev polynomials were the basis polynomials for interpolation in the original work by Patera[8]. This choice was motivated by the fact that expansions with Chebyshev polynomials have the same (exponential) convergence as Fourier series. An alternative to the Chebyshev SEM was developed by Maday and Patera[13], with the use of a Lagrange interpolation in combination with the GLL quadrature, leading to a diagonal structure of the mass matrix and this nodal lumping quadrature has also been termed as optimal lumping [14]. This diagonal mass matrix is a very significant advantage of Legendre spectral element method over classical FEMs, and over variant of SEM based on Chebyshev formulation, such as Priolo et al [15].

The SEM was used for acoustic wave equations by Zhu [16] and Degrande and Roeck [17]. Seriani [18] used three-dimensional SEM to simulate wave equation and element by element method was used. Mehdizadeh and Paraschivoiu [19] investigated a two-dimensional Helmholtz's equation by SEM. Komatitsch and Tromp [9] introduced SEM for three-dimensional seismic wave propagation. Komatitsch and Barnes [20] used SEM for wave propagation near fluid-solid interface.

In this research, two dimensional Legendre spectral element methods is applied as an alternative to the finite element methods in the dam-reservoir interaction problem and efficiency and accuracy of both methods are compared.

## 2. The Coupled Dam-Reservoir Problem

The dam-reservoir system can be classified as a coupled field problem in which two physical domains of fluid and structure interact at the interface plane. In such a system, the presence of interaction imposes that the time response of both subsystems must be evaluated simultaneously. Different techniques have been proposed for the simultaneous solution of the dam-reservoir interaction problem using the finite element approach. Displacement was chosen as response variable for the structure while pressure may be chosen as a response variable for the fluid (Lagrangian- Eulearian approach). In this case, the equation of motion of the coupled dam-reservoir system is unsymmetrical and stiffness proportional damping (Rayleigh damping) is used.

### 2.1. Governing equations for fluid and boundary conditions

Neglecting the internal viscosity, and assuming the water to be linearly compressible with a small amplitude irrotational two-dimensional movement, the hydrodynamic

pressure distribution in the reservoir system is governed by the Helmholtz equation:

$$\nabla^2 P(x, y, t) = \frac{1}{c^2} \ddot{P}(x, y, t) \quad (1)$$

where  $P(x, y, t)$  is the hydrodynamic pressure distribution in excess of the hydrostatic pressure,  $c$  is the acoustic wave velocity in water,  $t$  is the time variable ( see Fig. 1).

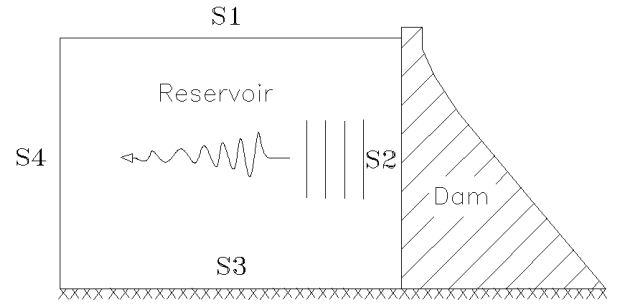


**Fig. 1** The dam-reservoir interaction system with reservoir domain boundaries

### 2.2. Finite element modeling of the reservoir

Using the finite element discretization of the fluid domain and the Galerkin formulation of Eqn. (3), the wave equation can be written in the following matrix form:

$$[E1]\{\ddot{P}\} + [H]\{P\} = \{F\} \quad (2)$$

where  $E1_{ij} = \sum E1_{ij}^e$ ,  $H_{ij} = \sum H_{ij}^e$  and  $F_{ij} = \sum F_{ij}^e$ . The coefficients  $E1_{ij}^e$ ,  $H_{ij}^e$  and  $F_{ij}^e$  for an individual element are determined using the following expressions:

$$E1_{ij}^e = \frac{1}{c^2} \int_{A_e} N_i N_j dA \quad (3)$$

$$H_{ij}^e = \int_{A_e} \left( \frac{\partial N_i}{\partial x} \frac{\partial N_j}{\partial x} + \frac{\partial N_i}{\partial y} \frac{\partial N_j}{\partial y} \right) dA \quad (4)$$

$$F_i^e = \int_{s_e} N_i \frac{\partial P}{\partial n} ds = \sum_{b=1}^4 \int_{s_b} N_i \frac{\partial P}{\partial n} ds \quad (5)$$

where  $N_i$  is the element shape function,  $A_e$  is the element area and  $s_b$  is the prescribed length along the side of boundary elements as shown in Fig. 1.

The hydrodynamic pressure distributions within the domain may be obtained by solving Eqn. (1) with the following boundary conditions:

(1) At the free surface: considering the free surface wave, the boundary condition at the free surface is written as.

$$\frac{\partial P(x, y, t)}{\partial n} = -\frac{1}{g} \ddot{P}(x, y, t) \quad (6)$$

$$\int_{s_1} N_i \frac{\partial P}{\partial n} ds = \left[ \frac{1}{g} \int_{s_1} N_i N_j ds \right] \{\ddot{P}\} = [E2] \{\ddot{P}\} \quad (7)$$

(2) At the dam-reservoir interface:

$$\frac{\partial P(x, y, t)}{\partial n} = -\rho a_n(x, y, t) \quad (8)$$

$$\int_{s_2} N_i \frac{\partial P}{\partial n} ds = \rho \left[ \int_{s_2} N_i n N_j ds \right] \{\ddot{u}_{tot}\} = \rho [Q^T] \{\ddot{u}_{tot}\} \quad (9)$$

where  $\rho$  is the density of water and  $a_n(x, y, t)$  is the component of acceleration on the boundary along the direction of the inward normal  $n$ .  $\{\ddot{u}_{tot}\}$  is the total acceleration of dam grids and  $Q$  is the coupling matrix between dam and reservoir.

(3) At the reservoir bottom:

For simplification of the analytical procedures, the bottom of the reservoir is generally considered to be rigid, which does not represent the actual behavior of the system. The absorption of the pressure waves by sedimentary material in the reservoir bottom is an important factor that may significantly affect the magnitude of the hydrodynamic force on the dam. Simple absorption boundary condition is used in the current work using the following expression [6]:

$$\frac{\partial P(x, y, t)}{\partial n} = -\rho a_n(x, y, t) - q \dot{P}(x, y, t) \quad (10)$$

where  $q$  is a damping coefficient which is the fundamental parameter characterizing the effects of the reservoir bottom materials and it defines as [6]:

$$q = \frac{1}{c} \left( \frac{1 - \alpha}{1 + \alpha} \right) \quad (11)$$

in which  $\alpha$  is the ratio of the amplitude of the reflected hydrodynamic pressure wave to the amplitude of avertically propagating pressure wave incident on the reservoir bottom.

$$\int_{s_3} N_i \frac{\partial P}{\partial n} ds = \left[ q \int_{s_3} N_i N_j ds \right] \{\dot{P}\} = [A2] \{\dot{P}\} \quad (12)$$

where  $A2$  is the refraction damping matrix.

(4) Truncation boundary condition:

In the finite element modeling of the reservoir a suitable boundary condition should be applied along the truncation surface. Sommerfeld boundary condition is the most commonly used approach which is based on the assumption that at a far distance from the dam face, the outgoing waves can be considered as plane waves. This boundary condition is the most suitable for the time domain analysis. Consequently in the present analysis, the Sommerfeld radiation boundary condition is used as the following formulas:

$$\frac{\partial P(x, y, t)}{\partial n} = -\frac{1}{c} \dot{P}(x, y, t) \quad (13)$$

$$\int_{s_4} N_i \frac{\partial P}{\partial n} ds = \left[ \frac{1}{c} \int_{s_4} N_i N_j ds \right] \{\dot{P}\} = [A1] \{\dot{P}\} \quad (14)$$

where  $A1$  is the radiation damping matrix. The physical meaning of the boundary condition is equivalent to adding dampers to absorb the outgoing waves in the truncation boundary.

### 2.3. Coupling of dam and reservoir equations

Finally the dam-reservoir interaction is a classic coupled problem, which contains two differential equations of the second order. The equations of the dam structure and the reservoir can be written in the following form:

$$[M]\{\ddot{U}\} + [C]\{\dot{U}\} + [K]\{U\} = \{F1\} - [M]\{\ddot{u}_g\} + [Q]\{P\} \quad (15)$$

$$[E]\{\ddot{P}\} + [A]\{\dot{P}\} + [H]\{P\} = \{F2\} - \rho [Q]\{\ddot{u}_{tot}\} \quad (16)$$

Where  $[M]$ ,  $[C]$  and  $[K]$  are the mass, damping and stiffness matrices of the dam and  $[E]=[E1]+[E2]$ ,  $[A]=[A1]+[A2]$  and  $[H]$  are the matrices representing the mass, damping and stiffness of the reservoir, respectively.  $[Q]$  is the coupling matrix,  $\{F1\}$  is the vector of body force and hydrostatic force,  $\{F2\}$  is the component of the force due to acceleration at the boundaries of the dam-reservoir and dam-foundation.  $[P]$ ,  $[U]$  and  $\{\ddot{u}_g\}$  are the vectors of the hydrodynamic pressures of the reservoir, the displacements of the dam and the ground accelerations, respectively.  $\{\ddot{u}_{tot}\} = \{\ddot{U}\} + \{\ddot{u}_g\}$  and  $\rho$  is the density of the fluid. The over-dot represents the time derivative.

## 3. Solution of the Coupled Equations

### 3.1. Staggered method

There are different approaches to solve the coupled field problems. Three categories of the approaches are field elimination, simultaneous solution and partitioned solution. The main disadvantage of the first two categories of solution occurs from the difficulties encountered in using available software, while the partitioned solution has the capability of using existing software for each subsystem. The staggered solution is a partitioned solution procedure that can be organized in terms of sequential execution of a single-field analyzer [21]. A simple concept of this method at any time step as follows:

1. An arbitrary  $P_{init}$  is substituted into Eqn. (15) to calculate  $\ddot{U}$ .

2. Calculated  $\ddot{U}$  is introduced in Eqn. (16) to obtain  $P$ .

3. If  $P - P_{init}$  don't be lower than a reasonable tolerance,  $P$  is substituted again in the Eqn. (15) then the new  $\ddot{U}$  is calculated to obtain new  $P$  and the cycle of 1, 2 continues until convergence.

However it is better that introduce previous time step  $P$

as  $P_{init}$  for rapid convergence at the initial of each time step.

### 3.2. Time-stepping scheme of the coupled equations

Direct integration method is used to find the displacement and hydrodynamic pressure at the end of the time increment  $i+1$  given the displacement and hydrodynamic pressure at time  $i$ . Considering the stability of the algorithm, an implicit Newmark method is adopted in this study. In the interval of  $t \sim t + \Delta t$ , the assumption as follows is used:

$$\dot{u}_{t+\Delta t} = \dot{u}_t + [(1 - \delta)\ddot{u}_t + \delta\ddot{u}_{t+\Delta t}]\Delta t \quad (17)$$

$$u_{t+\Delta t} = u_t + \dot{u}_t\Delta t + [(0.5 - \alpha)\ddot{u}_t + \alpha\ddot{u}_{t+\Delta t}]\Delta t^2 \quad (18)$$

$\alpha$  and  $\delta$  are parameters determined by the requirement of scheme stability and integration accuracy. It can be proved that the scheme is absolutely stable for time step when  $\alpha \geq 0.25(0.5 + \delta)^2$  and  $\delta \geq 0.5$ [15]. Thus, the recurrence formula can be obtained:

$$\begin{aligned} & \left(K + \frac{1}{\alpha\Delta t^2}M\right)u_{t+\Delta t} \\ &= R_{t+\Delta t} + M\left[\frac{1}{\alpha\Delta t^2}u_t + \frac{1}{\alpha\Delta t}\dot{u}_t + \left(\frac{1}{2\alpha} - 1\right)\ddot{u}_t\right] \\ &+ C\left[\frac{\delta}{\alpha\Delta t}u_t + \left(\frac{\delta}{\alpha} - 1\right)\dot{u}_t + \left(\frac{\delta}{2\alpha}\right)\Delta t\ddot{u}_t\right] \end{aligned} \quad (19)$$

and  $\ddot{u}_0$  on the initial step is obtained by:

$$\ddot{u}_0 = M^{-1}(R_0 - Ku_0 - C\dot{u}_t) \quad (20)$$

Although the integration method is absolutely stable, the time step has effect on the numerical accuracy, which suggests that the time step should be small enough to assurance certain degree of accuracy.

## 4. Spectral Element Method (SEM)

The spectral element combines the advantages of the Galerkin spectral method with of those in the finite element method. This means that, like in the finite element methods, the domain is divided into  $N_{el}$  elements to gain the flexibility and matrix sparsity of the finite elements:

$$\bar{\Omega} = \bigcup_{e=1}^{N_{el}} \bar{\Omega}_e \bigcap_{e=1}^{N_{el}} \Omega_e = \emptyset \quad (21)$$

At the same time, the degree of the polynomials  $N$  in each sub domain is sufficiently high to preserve the high accuracy and low storage of spectral methods. Convergence is obtained either by increasing the degree of the polynomials or by the number of elements  $N_{el}$ . For  $N_{el} = 1$  a spectral Galerkin method is achieved. If  $N = 1$  or  $N = 2$  a standard Galerkin finite element method is obtained based on linear and quadratic elements respectively.

In each element, the solution is approximated with

Legendre based polynomials of order  $N$  in each spatial direction. The basic functions are typically high-order Lagrange interpolation polynomials through the local Gauss-Lobatto-Legendre integration points defined per element. A parent element is introduced in practice to simplify the spectral element implementation. A nodal basis for the parent element is built by Lagrangian basis polynomials associated with a tensor product grid of Gauss-Lobatto-Legendre (GLL) nodes. The GLL grid nodes in each direction are the roots of the polynomials:

$$(1 - x^2)P'_N(x) = 0 \quad (22)$$

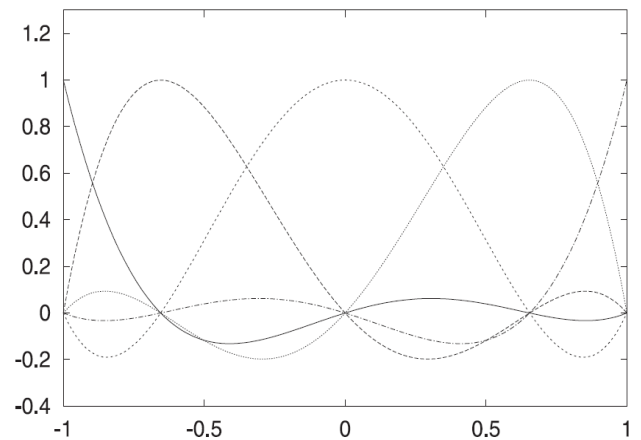
where  $P_N(x)$  is the Legendre polynomial of degree  $N$  in  $[-1, 1]$ :

$$\begin{aligned} P_0(x) &= 1, P_1(x) = x, \\ P_{n+1}(x) &= \frac{2n+1}{n+1}xP_n(x) - \frac{n}{n+1}P_{n-1}(x) \quad n \geq 1 \end{aligned} \quad (23)$$

The basic functions are constructed as a set of Lagrange interpolants. The Lagrange interpolants associated with the  $i$ th and  $j$ th grid node is defined as:

$$h_{ij}(r, s) = \prod_{\substack{m=0 \\ m \neq i}}^N \frac{(r - \bar{r}_m)}{(\bar{r}_i - \bar{r}_m)} \prod_{\substack{n=0 \\ n \neq j}}^N \frac{(s - \bar{s}_n)}{(\bar{s}_j - \bar{s}_n)} \quad (24)$$

where  $r$  and  $s$  are the coordinate system in the parent element, and  $\bar{r}_i$  is the coordinate of the  $i$ th grid node in the direction of  $r$  and similarly  $\bar{s}_j$  is the coordinate of the  $j$ th grid node in the direction of  $s$ . An example of such a grid is shown in Fig. 2 for a fourth-order polynomial space. The  $N+1=5$  GLL points can be distinguished along the horizontal axis. All Lagrange polynomials are, by definition, equal to 1 or 0 at each points. Note that the first and last points are exactly -1 and 1. Generally the GLL points are closer together at the edges and are further apart at the center of an element. In the global grid, points lying on edges or corners are shared between the elements. The contributions to the global system from each element sharing a grid point are summed up in the assembly stage.



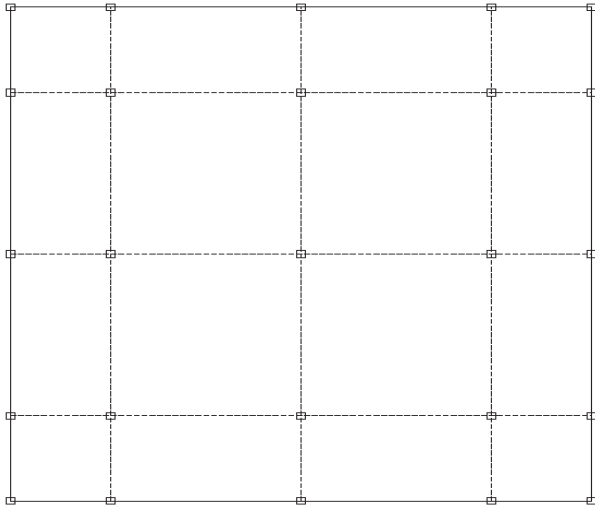


**Fig. 2** Lagrange interpolants of degree  $N=4$  on reference segment  $[-1,1]$  (top) and corresponding SEM element (bottom)

The shape function of the elements can be defined in terms of low-degree Lagrange polynomials. In a traditional FEM, low-degree polynomials are also used as basis-functions for the representation of the field variables on the elements. In a SEM, on the other hand, a higher-degree Lagrange interpolant is used to express functions on the elements. Therefore, spectral elements are sub parametric, because the interpolant used to describe the geometry is of lower order than the interpolant used to define the field variable.

#### 4.1. Numerical integration

The integrals in weak formulation of the problem have to be evaluated by means of a numerical quadrature. The integrands appearing in the SEM integrals involve higher order polynomials. To evaluate these integrals, quadrature rules are more practical. In the FEM Gauss-Legendre quadrature is frequently used for this purpose. In SEM, GLL quadrature points, shown in Fig. 2 for a parent element, are used to numerically evaluate the integrals. The advantage of using the same points both for defining basis functions and for the numerical quadrature is the convenient evaluation of the Lagrange interpolants at the grid points:

$$\int_{-1}^1 \int_{-1}^1 f(r,s) dr ds \approx \sum_{j=0}^N \sum_{k=0}^N w_j w_k f(r_j, s_k) \quad (25)$$

where  $r_j$  and  $s_k$  are the GLL quadrature nodes, and  $w_j$  and  $w_k$  are the weights associated with the quadrature nodes. The weights are given by:

$$w_j = \frac{2}{N(N+1)} \frac{1}{P_N^2(x)} \quad (26)$$

where  $P_N(x)$  is the Legendre polynomial of degree  $N$  introduced earlier.

The choice of a quadrature formula is determined by the requirement that the integration error has to be of the same order or smaller than the approximation error. In the case of the stiffness and mass matrices, the quantities to be integrated are polynomials of order  $2N - 2$  and  $2N$  respectively. This advocates a Gauss type formula associated with the Legendre polynomials because such a formula based on  $N + 1$  nodes is exact for polynomials of order  $2N + 1$ . It is very attractive to use a Gauss quadrature based on the Legendre-Gauss-Lobatto points in  $[-1, 1]$ . This choice combined with the basic functions introduced above would result in a diagonal mass matrix which is important in the context of iterative or time-dependent procedures. Moreover, in 2-D and 3-D cases it allows a significant decrease of the number of processes and storage necessities for the construction of the stiffness matrix. This quadrature is exact for the polynomials of order  $2N - 1$ . An error occurs because of the mass matrix of  $2N$  order, nevertheless the accuracy of the scheme is maintained [22]. Maday and Patera[13] proved that if the functions are analytical, this quadrature preserves the most attractive property of the spectral methods which is their exponential convergence.

## 5. Numerical Results

### 5.1. Basic parameters

The tallest monolith of the Pine flat concrete gravity dam, located in California, was chosen for the analysis. This particular dam was selected because it has been the subject of numerous experimental and theoretical studies. The dam structure has the crest length of 560 m and consists of 37 monoliths 15.2m wide, which the tallest of them is 122 m. The concrete is assumed to be homogeneous and isotropic, while water is considered as a compressible and inviscid fluid. In dam structure, Rayleigh damping method is used and its relevant coefficients are determined such that damping would be equivalent to 5% of critical damping for frequencies close to the first and third modes of vibration. The modulus of elasticity, unit weight and Poisson's ratio of concrete were taken as 2275MPa, 2500 kg/m<sup>3</sup> and 0.2, respectively. The dam is assumed to be in the case of plain stress. The velocity of pressure waves in water was taken as 1440m/s. The depth of the reservoir is 116.2 m. Static loading consists of weight and hydrostatic pressures which are applied initially. Thereafter, dynamic loading is considered. The finite and spectral element model of the dam-reservoir system is shown in Fig. 3.

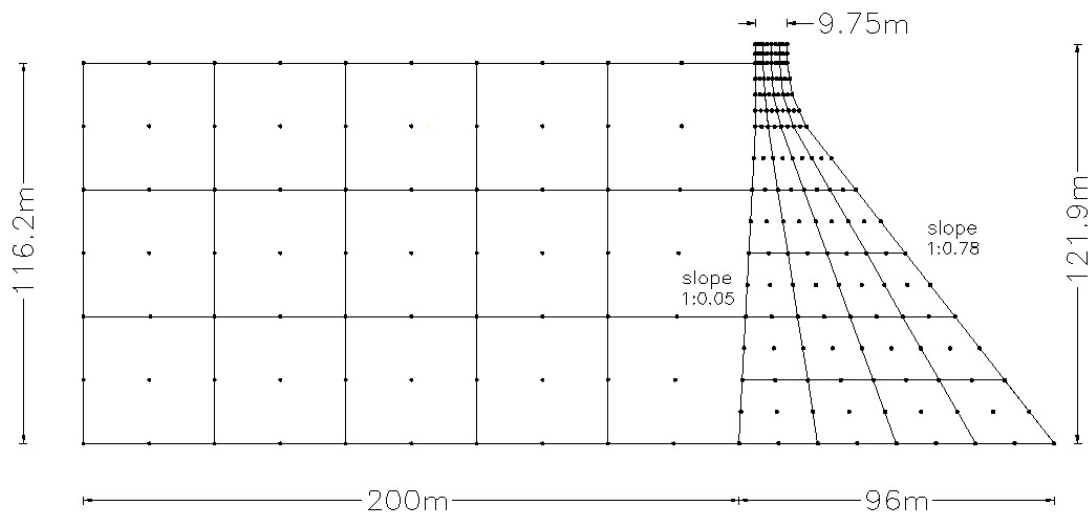


**Fig. 3** The finite and spectral element model of the dam-reservoir problem

Fig. 4 shows 10 sec. of the horizontal S69E component of the 21 July 1952 Taft Lincoln earthquake, Kern County site record, which is selected for seismic analysis. The ground motion has a peak acceleration of 0.157g and the

time step of 0.01 sec is chosen for the analysis. The integration parameters in the Newmark method were taken as  $\alpha=0.25$  and  $\delta=0.5$ .

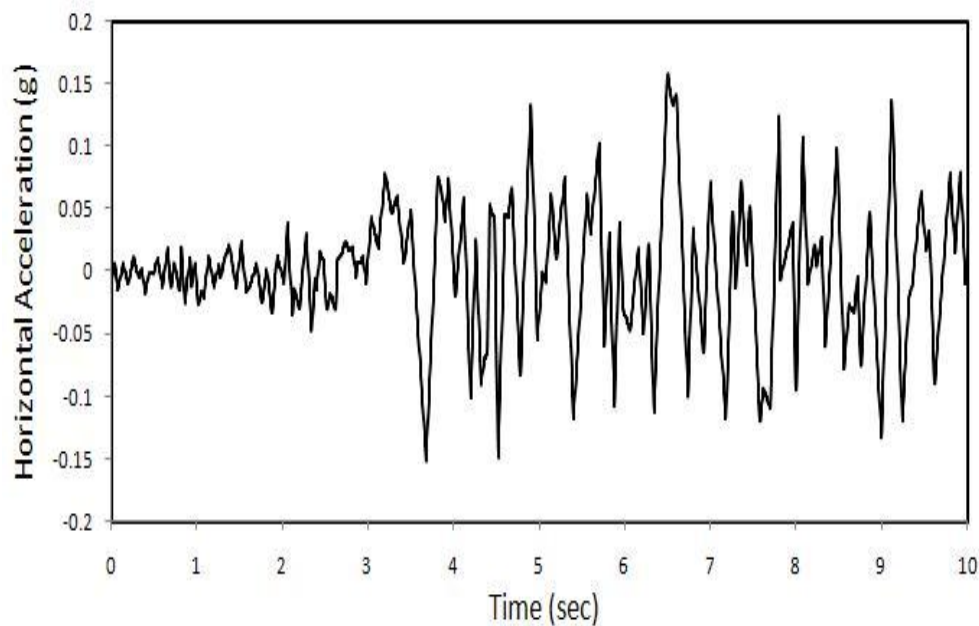


**Fig. 4** First 10 sec of the horizontal S69E component of 21 July 1952 Taft Lincoln earthquake, Kern County site record

A special code was developed to carry out the dynamic analysis of the system by using the two-dimensional FEM and SEM. Numerous studies have been done to choose the best geometry and element size in the dam and reservoir domain. Dam and reservoir domains are modeled by the same method (SEM or FEM) because the interaction matrix  $Q$  should be integrated by unit numerical quadrature rule. Length of the reservoir should be large enough to obtain accurate results by the conventional boundary conditions unless outgoing waves reflect to the reservoir domain and the results will not be accurate. Results from different analysis by various element sizes and polynomial degrees of the reservoir elements show that the square elements with equal grid numbers in two

directions induced the optimum time of the analysis and accurate results. Consequently 200 m length of the reservoir domain with 40 m of the element size is used in numerical modeling with the same height elements. In order to verify the results obtained from the developed code, different analyses are carried out and the results are compared to previous researches. The horizontal displacement at the dam crest obtained from this analysis and the results presented by Samii and Lotfi [23] are illustrated in Fig. 5. The initial nonzero crest displacement represents the deformation due to the weight of the dam and the hydrostatic pressure component. Good agreement is found between the responses as shown in Fig. 5.



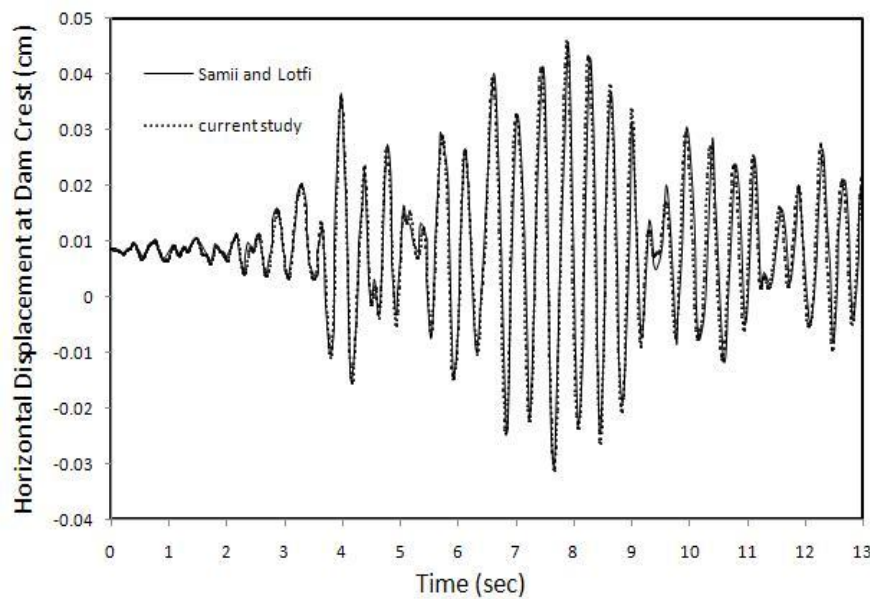


**Fig. 5** Comparison of the results for the horizontal displacement at the dam crest obtained from the present study and Samii and Lotfi

## 5.2. Dam only analysis

The dam only analysis without any interaction is carried out by FEM and SEM methods. The same results are obtained from the analysis under the static loads using both methods. The results of the seismic analysis corresponding to the maximum crest displacement and the natural frequency of the dam are presented in Table. 1.

It is demonstrated that although for linear elements the results indicates considerable discrepancies but for quadratic elements good agreement is achieved. In fact, the SEM uses powerful Spectral convergence to reach FEM rapidly by increasing of the degree of interpolation polynomial. The results for the displacement of the dam crest are presented in Fig. 6.

**Table 1** Comparison of the Dam crest displacement and natural frequency obtained by FEM and SEM

Method	FEM			SEM		
Elements type	Horizontal disp. (cm)	Vertical disp.(cm)	Natural Frequency (Hz)	Horizontal disp.(cm)	Vertical disp.(cm)	Natural Frequency (Hz)
Linear (N=1)	2.75	0.24	3.32	2.22	0.10	3.73
Quadratic (N=2)	3.68	0.52	3.14	3.67	0.52	3.14

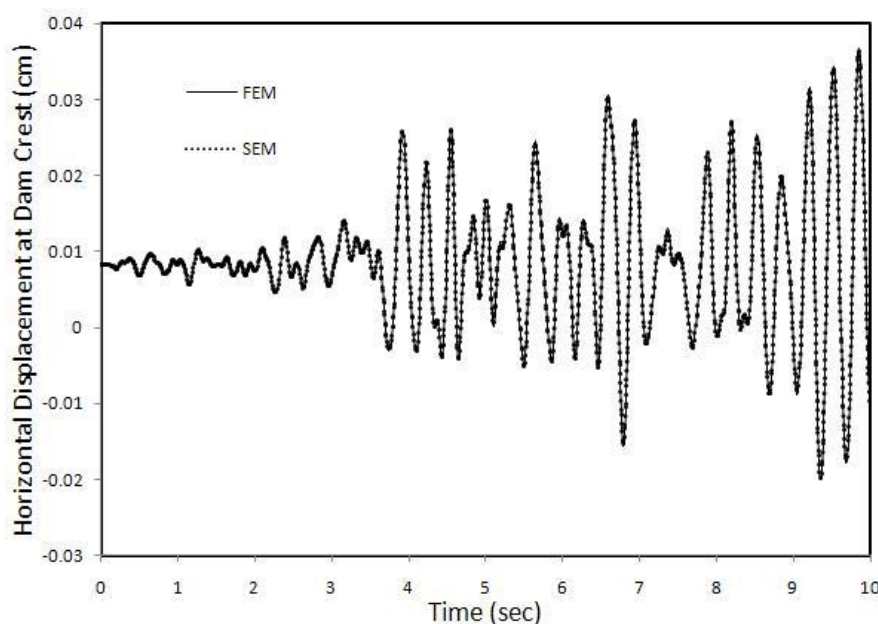


**Fig. 6** Comparison of the dam Crest displacement for dam only analysis

While good agreement between the results of both methods are achieved, less computational time are used by the SEM because of the diagonal mass and relatively more sparse stiffness matrix. It seems that for the large scale problems of the dynamic analysis of the structures such as dams, the SEM can be used as a good alternative to the FEM with ordinary mesh. Clearly the larger size of the structure is, the stronger SEM performs.

### 5.3. Coupled dam-reservoir analysis

The dam-reservoir discretized model which is used in the analysis is illustrated in Fig. 3. Reservoir bottom

absorption has a significant effect on the peak values of the dam crest displacement and the hydrodynamic pressure of the reservoir [24]. To observe the effect of the reservoir bottom absorption on the seismic response of dam-reservoir system, the same model with two different absorption values in considered. The variation of the crest displacement and hydrodynamic pressure at the dam heel due to Taft earthquake are shown in Fig. 7. As illustrated in Fig. 8, the peak values of the displacement and hydrodynamic pressure are reduced considering the absorptive reservoir bottom with  $\alpha=0.8$ . Therefore for more realistic condition,  $\alpha=0.8$  has been used in all analysis.

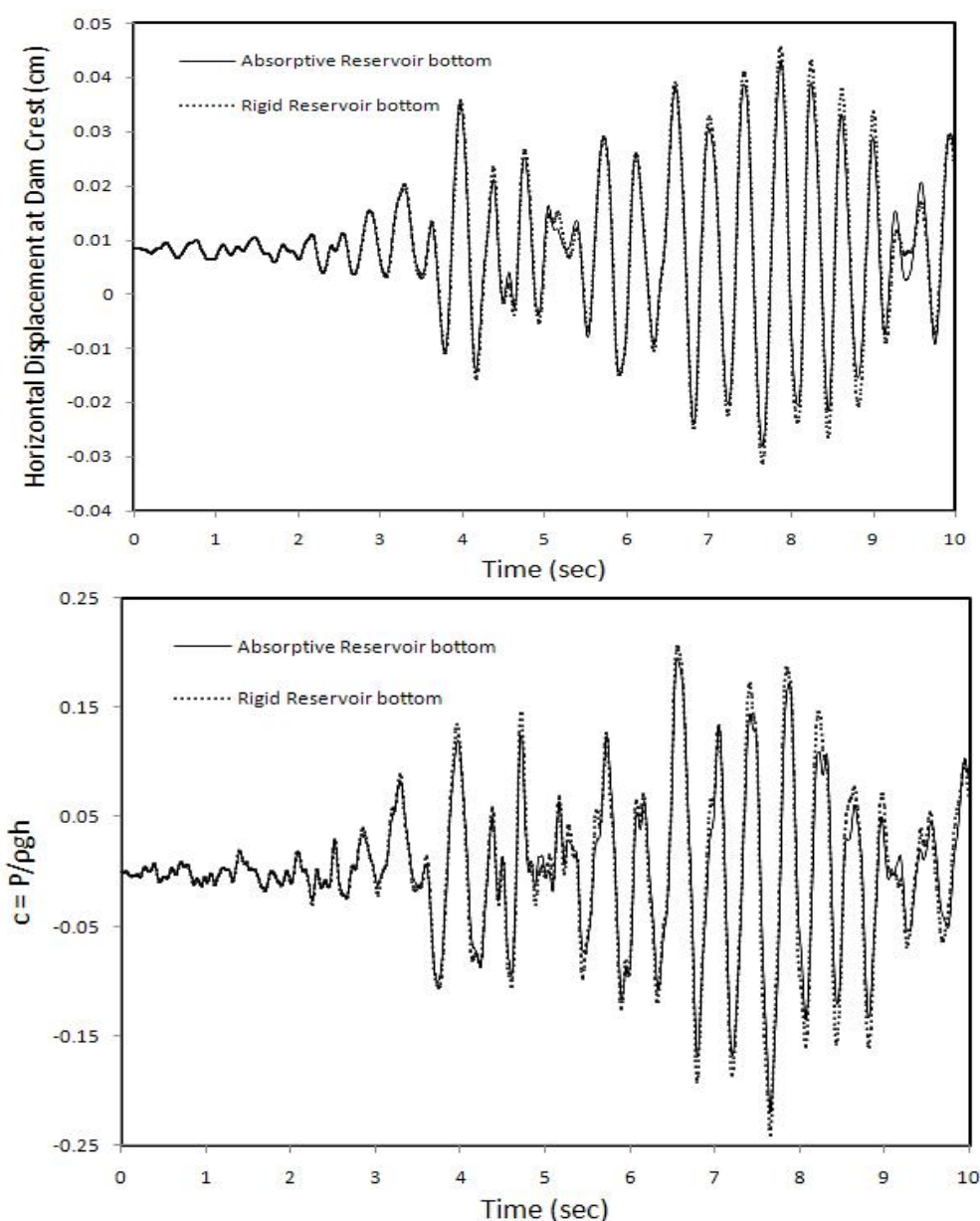


**Fig. 7** Effect of the reservoir bottom absorption on the horizontal displacement at the dam crest (top) and hydrodynamic pressure at the dam heel (bottom) due to Taft earthquake



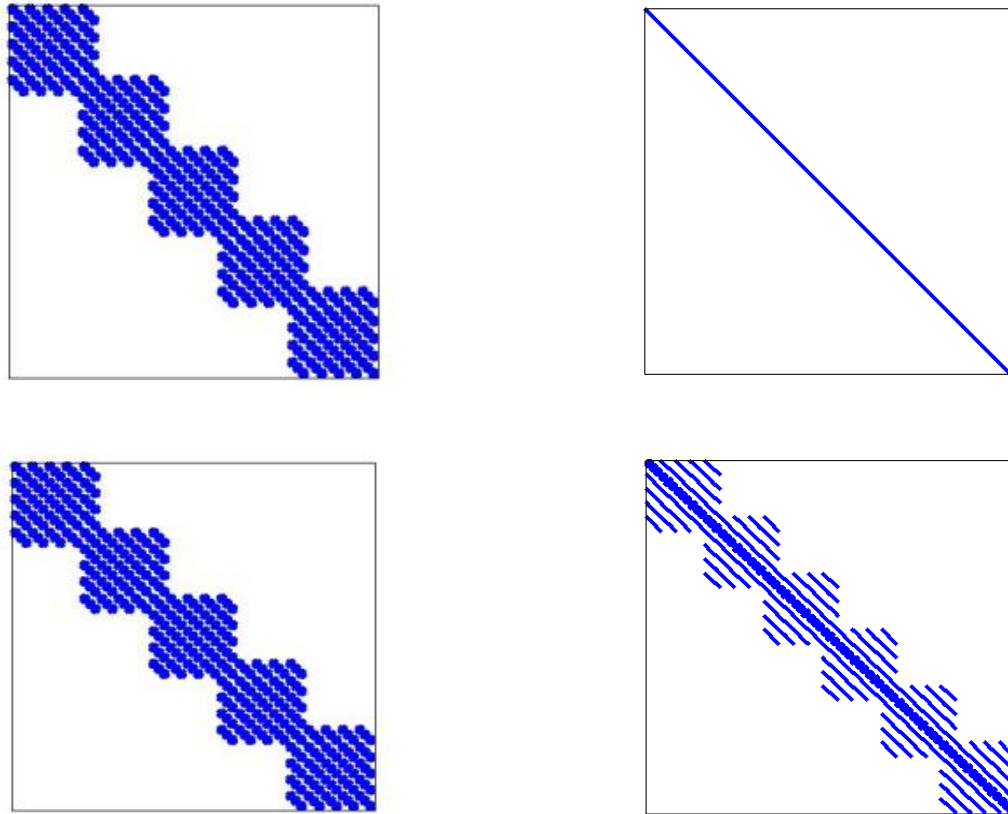


**Fig. 8** Comparison of the reservoir mass (top) and stiffness (bottom) matrix sparsities in the FEM and SEM

If the polynomial degree,  $N$ , is very high, greater than 10, the SEM is especially very accurate, but the computational requirements become unreasonable because of the size of the calculations related to the matrix multiplications involving the full stiffness matrix. Another problem in the case of a high degree is that irregularly spaced GLL numerical integration points become clustered toward the edges of each spectral element. The spacing between the first two GLL points varies approximately as  $(n^{-2})$ , and as a result of the small distance between these first two points, very small time steps have to be used to keep the explicit time-marching scheme stable, which drastically increases the cost of the Legendre SEM. Therefore, the rule of thumb is that for most wave propagation applications, polynomial degrees between

approximately 4 and 10 should be used in practice [9]. Table 2 indicates the maximum horizontal displacement of the dam crest and hydrodynamic pressure corresponding to the different  $N$ s. It is indicated as in the case of the dam only, although for the low order elements, the SEM causes poor results, for the high order elements the SEM reaches to the accuracy of the FEM rapidly. No significant changes on the accuracy of the results are obtained for the polynomials of 4 degrees and higher. Therefore  $N=4$  is used for different analysis of dam-reservoir system. It is important to mention that if we eliminate interior nodes of the elements and save the nodes along the edges of elements (serendipity type of elements), this is the same effect on the two methods and for simplicity, the elements with full nodes (Lagrangian type of elements) are used.

**Table 2** Maximum results of horizontal displacement at the dam crest and hydrodynamic pressure in the reservoir domain by FEM and SEM

Method		FEM		SEM	
N		$P_{max}$ (KPa)	$\Delta_{max}$ (cm)	$P_{max}$ (KPa)	$\Delta_{max}$ (cm)
N=1		214	3.53	218	3.40
N=2		237	4.32	232	4.16
N=3		239	4.45	240	4.41
N=4		240	4.48	240	4.46
N=5		240	4.48	240	4.47
N=6		240	4.48	240	4.47

In the SEM, all the integrals in the form of  $\int N_i N_j d\Omega$  can be evaluated as exact diagonal matrices consequently consistent mass matrix of the reservoir is evaluated as an exact diagonal mass matrix. Since Kroncker delta is not work in the derivative of Lagrange polynomials, stiffness matrix is not diagonal in the SEM but it's sparsity is more than which obtained by the FEM as shown in Fig. 8.

All four boundary conditions in the reservoir domain have the form of mass matrix,  $(\int N_i N_j d\Omega)$  and consequently evaluated by exact diagonal matrices by the SEM. For example matrix sparsity, corresponding to the reservoir bottom boundary condition, in both SEM and FEM is shown in Fig. 9.

Finally seismic analysis of dam-reservoir interaction system is performed by FEM and SEM. The comparison of the horizontal and vertical dam crest displacement are shown in Fig. 10. The maximum hydrodynamic pressures in the reservoir domain are indicated in Fig. 11. Excellent agreement are found for the results obtained from both methods.

In order to show the efficiency of the SEM relative to the FEM for dam-reservoir interaction problem, time consumptions of the analyses are compared for both methods with different order of the polynomials and presented in Fig. 12. The results shows that for the low order polynomials ( $N \leq 2$ ) no considerable difference for time consumption of the analysis is obtained. For higher order polynomials ( $N > 3$ ) a significant less CPU time (e.g. 1/6 for  $N=6$ ) is obtained for the SEM in comparison with the FEM. The diagonal mass and mass type matrices are very significant advantages of the Legendre spectral element method, using Lagrange interpolation in combination with the GLL quadrature, over classical FEM and consequently lead to a significant reduction in complexity of iterative methods. Besides, the more sparse stiffness matrix of the SEM allows a dramatic decrease for construction and storage requirements rather than the FEM. On the other hand higher order FEM with Lagrange

polynomials induces more parasite terms with substantially increases the convergence time. This is a big advantage of the SEM over the FEM especially for the higher order elements of the large scale systems.

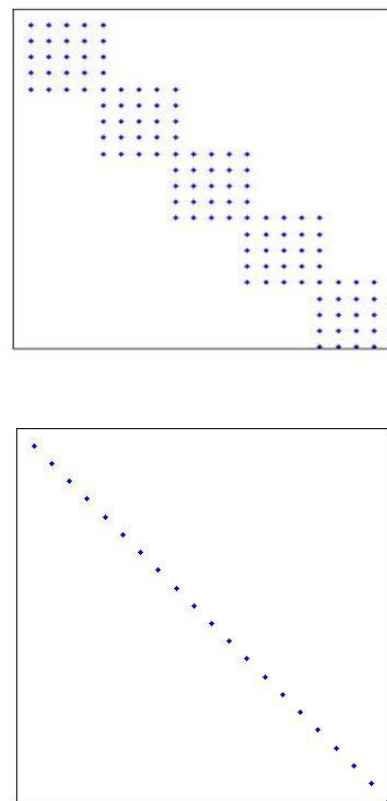


**Fig. 9** Comparison of the reservoir bottom damping matrix sparsity in the FEM (top) and SEM (bottom)

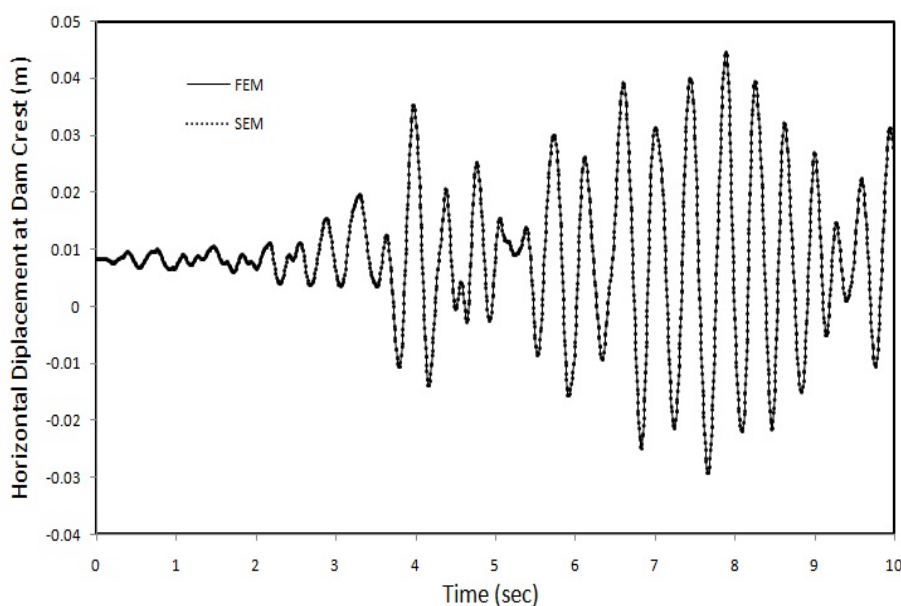


**Fig. 10** Comparison of the horizontal displacement at the dam crest considering the reservoir interaction effect

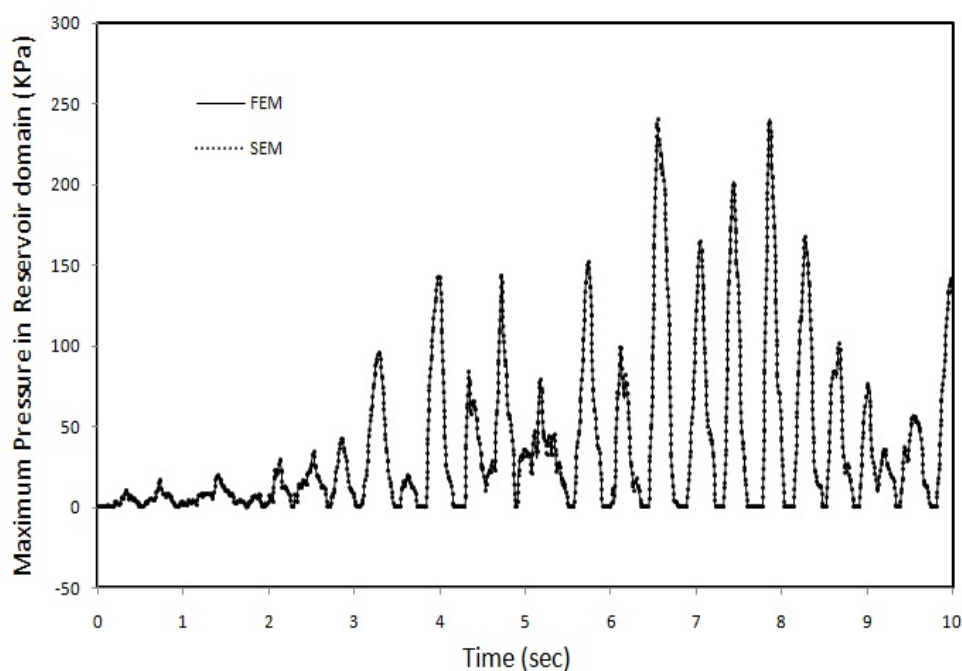


**Fig. 11** Comparison of the maximum hydrodynamic pressure in the reservoir domain

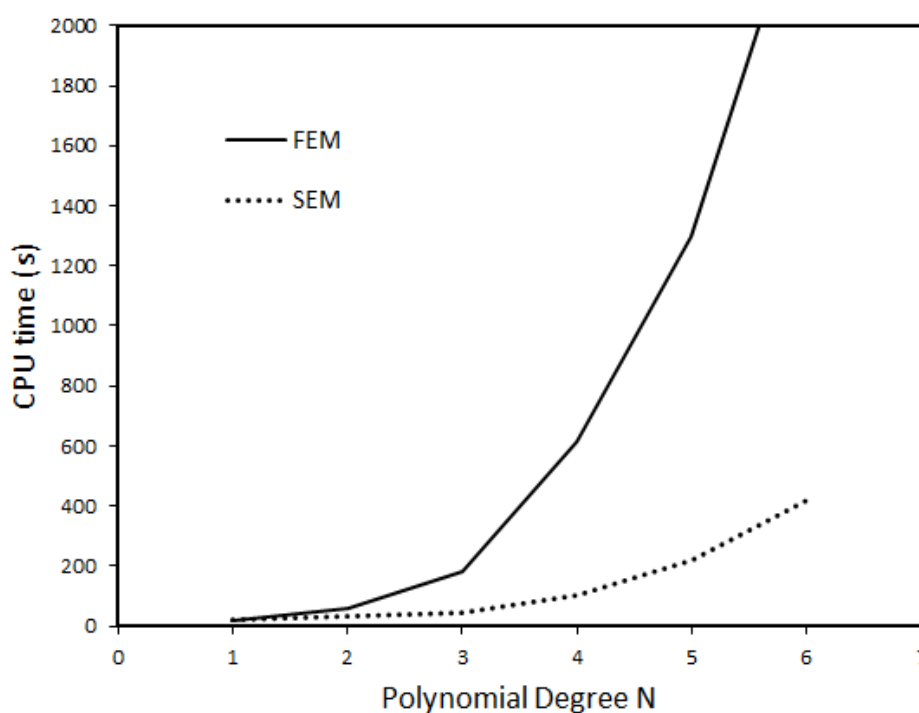


**Fig. 12** Comparison of the CPU time for the FEM and SEM

## 6. Conclusion

The dam–reservoir interaction problem was studied in the time domain by FEM and SEM. A special code was developed to carry out the dynamic analysis of the system by using two-dimensional elements. In order to verify the accuracy of the developed code comparison of the obtained results and previous researches were performed and good agreements were obtained. For lower order elements, the SEM causes poor results in comparison with

the FEM. Spectral convergence causes the SEM results converge to the FEM rapidly by increasing the degree of interpolation polynomials. The results indicate that for higher order elements the SEM is better alternative in the seismic analysis of the dam-reservoir interaction rather than the FEM because of the following reasons. (1) In the SEM all boundary conditions of the reservoir domain are evaluated by the exact diagonal matrices. (2) Diagonal mass matrices are obtained for both the dam and reservoir domains in the SEM. (3) Stiffness matrices of both the dam and reservoir systems are more sparse in the SEM

than FEM. (4) Less significant time consumption of the analysis were obtained in the SEM for higher order elements especially for the large scale systems (such as dam-reservoir) in comparison with the FEM.

**Acknowledgements:** The authors wish to thank Dr. K. Koohestani, A. Samii, C. Zhu and O. Z. Mehdizadeh for their helpful comments during this research.

## References

- [1] Westergaard HM. Water pressure on dams during earthquake, Transactions of the American Society of Civil Engineers, ASCE, 1933, Vol. 98, pp. 418-433.
- [2] Chopra AK. Hydrodynamic pressures on dams during earthquakes, Journal of Engineering Mechanics, 1967, No. EM6, Vol. 93, pp. 23-205.
- [3] Chakrabarti P, Chopra AK. Earthquake analysis of gravity dams including hydrodynamic interaction, Earthquake Engineering and Structural Dynamics, 1973, Vol. 2, pp. 60-143.
- [4] Chopra AK, Chakrabarti P. Earthquake analysis of concrete gravity dams including dam-water-foundation rock interaction, Earthquake Engineering and Structural Dynamics, 1981, No. 4, Vol. 9, pp. 83-363.
- [5] Hall JF, Chopra AK. Two-dimensional dynamic analysis of concrete gravity and embankment dams including hydrodynamic effects, Earthquake Engineering and Structural Dynamics, 1982, Vol. 10, pp. 32-325.
- [6] Fenves G, Chopra AK. Earthquake analysis of concrete gravity dams including bottom absorption and dam - water - foundation rock interaction, Earthquake Engineering and Structural Dynamics, 1984, Vol. 12, pp. 663-683.
- [7] Sharan SK. Finite element modeling of infinite reservoirs, Journal of Engineering Mechanics, 1985, No. 12, Vol. 111, pp. 69-1457.
- [8] Patera TA. A spectral element method for fluid dynamics: laminar flow in a channel expansion, Journal of Computational Physics, 1984, Vol. 54, pp. 468-488.
- [9] Komatitsch D, Tromp J. Introduction to the spectral element method for three-dimensional seismic wave propagation, Geophysical Journal International, 1999, Vol. 139, pp. 806-822.
- [10] Sprague MA, Geers TL. Legendre spectral elements for structural dynamics analysis, Communication in Numerical Methods in Engineering, 2008, Vol. 24, pp. 1953-1965.
- [11] Lee U, Kim J, Leung AYT. Spectral element method in structural dynamics, Shock & Vibration Digest, 2000, No. 32, Vol. 6, pp. 451-465.
- [12] Trefethen LN. Spectral Methods in MATLAB: Software. Environments, Tools, SIAM, Philadelphia, PA, 2000.
- [13] Maday Y, Patera TA. Spectral element methods for the incompressible Navier-stokes equations, State-of-the-Art Surveys on Computational Mechanics, ASME, New York, 1989.
- [14] Bathe KJ. Finite Element Procedures, second ed., Prentice-Hall, Englewood Cliffs, NJ, 1995.
- [15] Priolo E, Seriani G. A numerical investigation of chebyshev spectral element method for acoustic wave propagation, Proceedings of the 13th IMACS Conference Comparat. Appl. Math, 1991.
- [16] Zhu C, Qin G, Zhang J. Implicit chebyshev spectral element method for acoustics wave equations, Finite Elements in Analysis and Design, 2011, No. 2, Vol. 47, pp. 184-194.
- [17] Degrande G, Roeck GD. A spectral element method for two-dimensional wave propagation in horizontally layered saturated porous media, Computer and Structures, 1992, Vol. 44, pp. 717-728.
- [18] Seriani G. A parallel spectral element method for acoustic wave modeling, Journal of Computational Acoustics, 1997, Vol. 5, pp. 53-69.
- [19] Mehdizadeh OZ, Paraschivou M. Investigation of a two-dimensional spectral element method for Helmholtz's equation, Journal of Computational Physics, 2003, Vol. 189, pp. 111-129.
- [20] Komatitsch D, Barnes C, Tromp J. Wave propagation near a fluid-solid interface: A spectral element approach, Geophysical Journal International, 2000, No. 2, Vol. 65, pp. 623-631.
- [21] Ghaemian M, Ghobrah A. Staggered solution schemes for dam-reservoir interaction, Journal of Fluids and Structures - Elsevier, 1998, Vol. 12, pp. 933-948.
- [22] Cohen GC. Higher-Order Numerical Methods for Transient Wave Equations, Springer, Berlin, 2002.
- [23] Samii A, Lotfi V. Comparison of coupled and decoupled modal approaches in seismic analysis of concrete gravity dams in time domain, Finite Elements in Analysis and Design, 2007, No. 13, Vol. 43, pp. 1003-1012.
- [24] Gogoi I, Maity D. A novel procedure for determination of hydrodynamic pressure along upstream face of dams due to earthquakes, Computer and Structures, 2010, Vol. 88, pp. 539-548.